Electronic Supplementary Material (ESI) for Chemical Communications


# Supporting Information

## Formation of 'Single Wall' $TiO_2$ Nanotubes with Significantly Enhanced Electronic Properties for Higher Efficiency Dye-sensitized Solar Cells

**Hamed Mirabolghasemi[#], Ning Liu, Kiyoung Lee, Patrik Schmuki***

*Department of Material Science WW-4, LKO, University of Erlangen-Nuremberg, Martensstrasse 7, 91058 Erlangen, Germany*

[#] *On leave from Department of Materials Science & Engineering, (lab of Prof. Daniel John Blackwood), National University of Singapore, 7 Engineering Drive 1, Singapore*

*Corresponding author. Tel.: +49 91318517575, fax: +49 9131 852 7582

Email: schmuki@ww.uni-erlangen.de

**Experimental:**

As substrates for any type of $TiO_2$ nanotube growth we used titanium foils (99.6% purity, Goodfellow) with a thickness of 0.1 mm. Prior to tube formation the foils were cleaned by sonication in acetone and ethanol followed by rinsing with deionized (DI) water and drying in a nitrogen stream. To perform electrochemical $TiO_2$ nanotube formation, the foils were anodized using a power supply (Voltcraft VLP 2403 pro) in a two electrode configuration with a counter electrode made from platinum gauze. The typical electrolyte for double wall $TiO_2$ nanotubes was prepared from ethylene glycol (EG, Sigma–Aldrich, containing less than 0.2 wt% $H_2O$), with addition of 1 M DI $H_2O$ and 0.1 M $NH_4F$ (Sigma–Aldrich, 98%). The best electrolyte for single wall $TiO_2$ nanotubes was found to be 1:1 EG and dimethyl sulfoxide (DMSO, Sigma–Aldrich, containing less than 0.2 wt% $H_2O$) by volume ratio, containing 1.5 M deionized water and 0.1 M $NH_4F$ (see Table S1).

To achieve a defined tube top morphology we used a two–step anodization approach, where the first anodization was carried out at 60V for 60 min in the EG/$H_2O$/$NH_4F$ electrolyte at room temperature, and then the layer was removed by strong sonication. Subsequently the double wall nanotubes were grown in the condition as in the first step for 60 min in the place of the removed nanotube film. The single wall nanotubes were grown in EG/dimethyl sulfoxide (DMSO)/$H_2O$/$NH_4F$ electrolyte at 60 V for 16 min at 60 $^oC$ during the anodization. The anodized foils then were kept at the same temperature in the electrolyte afterwards, for 50 minutes (post anodization treatment). Then the samples were cleaned with ethanol and DI water thoroughly and dried with a gentle stream of nitrogen gas. Under these conditions, double wall and single wall $TiO_2$ nanotube layers of a thickness of about 15 μm were obtained.

Thermal treatments of the nanotube layers were carried out in air using a Rapid Thermal Annealer (Jipelec JetFirst 100) at 500 ˚C with heating/cooling rates of 1 ˚C/s. The samples

were annealed at 500 ˚C for 1 h. A Hitachi FE-SEM S4800 was used for morphological characterization of the samples. The length of the nanotubes was directly obtained from SEM cross-sections. XRD patterns were collected using an X'pert Philips PMD diffractometer with a Panalytical X'celerator detector, using graphite-monochromatized CuKa radiation ($\lambda =$ 1.54056Å). Further morphological and structural characterization of the $TiO_2$ nanostructures was carried out with a TEM (Philips CM30 TEM/STEM). Additionally, an EDX (EDAX Genesis, fitted to SEM chamber) was also used for the chemical analysis.

For $TiCl_4$ treatments we used 0.2 M aqueous solutions of $TiCl_4$ prepared under ice-cooled conditions. The $TiO_2$ nanotube layers were then treated in a closed vessel at 70 ˚C for 30 min. Afterwards, the samples were washed with DI water and rinsed with ethanol to remove any excess $TiCl_4$ and finally dried in a $N_2$ stream. After the treatment, $TiO_2$ nanotube samples were annealed again at 450 ˚C for 30 min to crystallize attached nanoparticles.

For use in dye-sensitized solar cells, the samples were immersed in a 300 μM Ru-based dye (cis-bis (isothiocyanato) bis (2,2-bipyridyl 4,4-dicarboxylato) ruthenium(II) bis-tetrabutylammonium (D-719, Eversolar, Taiwan)) solution in a mixture of acetonitrile and tert-butyl alcohol (volume ratio: 1:1) for 3 days at 40 ˚C. After dye-sensitization, the samples were rinsed with acetonitrile to remove non-chemisorbed dye.

To evaluate the photovoltaic performance, the sensitized samples were sandwiched together with a Pt coated fluorine-doped glass counter electrode (TCO22-15, Solaronix) using a polymer spacer (Surlyn, Dupont). An electrolyte (Iodolyte R50, Solaronix) was introduced into the space between the sandwiched cells. The current-voltage characteristics of the cells were measured under simulated AM 1.5 (100 $mW/cm^2$) illumination provided by a solar simulator (300 W Xe with optical filter, Solarlight), applying an external bias to the cell and measuring the generated photocurrent with a Keithley model 2420 digital source meter.

Dye desorption measurements of the dye sensitized $TiO_2$ layers were carried out by immersing the samples in 5 ml of 10 mM KOH for 1 day. The concentration of fully desorbed

dye was measured spectroscopically (Lambda XLS UV/VIS spectrophotometer, PerkinElmer) at 520 nm. Intensity modulated photovoltage and photocurrent spectroscopy (IMVS and IMPS) measurements were carried out using modulated light (10 % modulation depth) from a high power green LED ($\lambda$ = 530 nm). The modulation frequency was controlled by a frequency response analyzer (FRA, Zahner) and the photocurrent or photovoltage of the cell was measured using an electrochemical interface (Zahner) and fed back into FRA for analysis. The light incident intensity on the cell was measured using a calibrated Si photodiode.

Solid-state conductivity measurements were carried and by evaporating a 300 nm thick Au dot, through a 2.1 mm wide opening in a shadow mask, onto the nanotube surface. Resistivity values were then obtained from I-V curves. The two point approach was found to be in line with reported results from four point measurements [1].

Thermogravimetric analysis (TGA) combined with a mass spectrometer (MS) was done using on a Netzsch STA 409 CD instrument equipped with a Skimmer QMS 422 mass spectrometer (MS/EI) while air annealing with a heating profile that consisted of 20 ˚C/min ramping to 600 ˚C, then holding for 60 min and then ramping back to RT with 20 ˚C/min. An initial scan revealed masses M = 44, 18, 40, 19 to be significantly desorbed during the measurement.

**Table S1** Anodization conditions that were screened to find the best single wall tubes.

**(a)** Electrolytes compositions, anodization conditions and the resulting morphology of nanotube arrays for EG:DMSO 1:2 and EG:DMSO 2:1 by volume.

| **Electrolyte Composition** | | | | **Anodization condition** | | | | |
|---|---|---|---|---|---|---|---|---|
| **EG** Vol. Ratio | **DMSO** Vol. Ratio | **F⁻(M)** | **H2O(M)** | **Time (min)** | **Voltage V** | **Temp (C)** | **Tubes' Length (µm)** | **Description** |
| 1 | 2 | 0.07 | 0.7 | 120 | 60 | 40 | 6 | ➢ Tube walls are rough.<br>➢ Porous nanostructure (tubes are not separated well).<br>➢ Small-hole size porous initiation layer on top. |
| | | | | 120 | 30 | 60 | 2 | |
| | | | | 120 | 60 | 60 | 60 | |
| | | | | 60 | 60 | 60 | 39 | |
| | | | | 40 | 60 | 60 | 28 | |
| | | | | 20 | 60 | 60 | 13.7 | |
| 1 | 2 | 0.1 | 1 | 10 | 60 | 60 | 15 | ➢ Nano-cubic shape particles seen on the top surface.<br>➢ Porous nanostructure (tubes are not separated well).<br>➢ Small-hole size porous initiation layer on top. |
| | | | | 15 | 60 | 60 | 18.8 | |
| | | | | 20 | 60 | 60 | 26 | |
| | | | | 30 | 60 | 60 | - | |
| | | | | 120 | 60 | 40 | 5.8 | |
| | | | | 180 | 60 | 40 | 6 | |
| 1 | 2 | 0.1 | 1.5 | 20 | 60 | 60 | 14.3 | ➢ Rough and grainy tube walls.<br>➢ Small-hole size porous initiation layer on top.<br>➢ Nano-cubic shape particles seen on the top surface. |
| 2 | 1 | 0.13 | 1.3 | 120 | 30 | 60 | Less than 4 | ➢ Nano- grass formed on top of the tubes. |
| | | | | 120 | 60 | 40 | 36 | |
| | | | | 120 | 60 | 60 | 45 | |
| 2 | 1 | 0.1 | 1 | 5 | 60 | 60 | 5.7 | ➢ Porous nanostructure (tubes are not separated well). |
| | | | | 10 | 60 | 60 | 11.7 | |
| | | | | 15 | 60 | 60 | 19 | |
| | | | | 40 | 60 | 40 | 27 | |
| | | | | 30 | 60 | 40 | 21 | |
| | | | | 20 | 60 | 40 | 15 | |
| 3 | 1 | 0.075 | 0.75 | 60 | 60 | RT | 15 | ➢ Very thick initiation layer on top. |
| | | | | 120 | 60 | RT | 17 | |

**(b)** Electrolytes compositions, anodization conditions and the resulting morphology of nanotube arrays for EG:DMSO 1:1 by volume.

| **Electrolyte Composition** | | | | **Anodization condition** | | | **Tubes' Length (µm)** | **Description** |
|---|---|---|---|---|---|---|---|---|
| **EG** Vol. Ratio | **DMSO** Vol. Ratio | **F⁻(M)** | **H2O(M)** | **Time (min)** | **Voltage V** | **Temp (C)** | | |
| 1 | 1 | 0.05 | 0.5 | 120 | 60 | RT | 11.6 | ➢ Thick porous initiation layer on top.<br>➢ Lower growth rate. |
| | | | | 240 | 60 | RT | 17.3 | |
| | | | | 120 | 60 | 60 | 30 | |
| | | | | 120 | 60 | 40 | 14.3 | |
| | | | | 120 | 40 | 40 | 8 | |
| 1 | 1 | 0.1 | 1 | 60 | 60 | RT | 7.35 | ➢ Porous nanostructure (tubes are not separated well). |
| | | | | 120 | 30 | 40 | 4 | |
| | | | | 120 | 30 | 60 | 2 | |
| | | | | 120 | 60 | 60 | More than 100 | |
| | | | | 120 | 60 | 40 | 30 | |
| | | | | 40 | 60 | 40 | 19 | |
| | | | | 30 | 60 | 40 | 16 | |
| | | | | 10 | 60 | 60 | 11 | |
| | | | | 60 | 60 | 60 | - | |
| | | | | 35 | 60 | 60 | 33 | |
| | | | | 10 | 60 | 60 | 15 | |
| | | | | 15 | 60 | 60 | 19 | |
| 1 | 1 | 0.1 | 1.5 | 15 | 60 | 60 | 13.7 | ➢ Tubes are well separated.<br>➢ The structure is double wall near to bottom after anodization.<br>➢ The structure is fully single wall after "Post anodization treatment" |
| | | | | 15 | 60 | 60 | 14 | |
| | | | | 16 | 60 | 60 | 16 | |

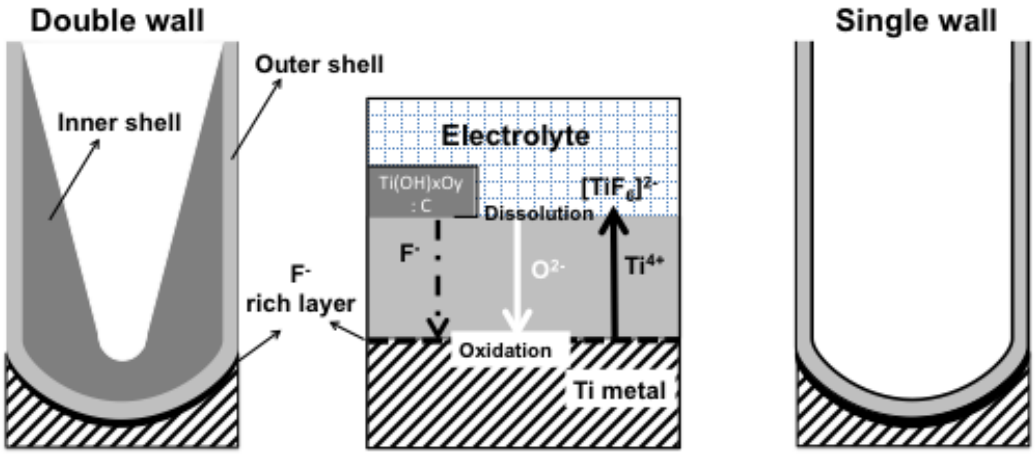


**Fig. S1** Schematic representation of formation of double wall (left) and single wall (right) $TiO_2$ nanotubes.

In order to explain the formation of the double layer oxide structure one may consider the nature of high field oxide formation during anodization (illustrated in the center of Fig. S1). Anodic $TiO_2$ can grow by two paths i) inward ion migration and ii) outward ion migration. 'Inward migration' oxide is based on $O^{2-}$ ions migrating from the solution/oxide interface towards the metal/oxide interface, where they react with $Ti^{4+}$ species formed at the metal/oxide interface. Oxide that grows by this reaction typically forms pure $TiO_2$ layers. 'Outward migration' oxide is formed by $Ti^{4+}$ that migrates outwards to the solution interface. The $Ti^{4+}$ arriving at the solution interface may react with the environment ($H_2O$) to form $TiO_2$ of a partially hydrated composition or alternative, it may be solvatized (e.g., as $TiF_6^{2-}$). Oxide or oxy-hydroxide layers formed by reaction of $Ti^{4+}$ with water are more of a precipitate nature, which also typically leads to encapsulation of electrolyte species and adsorbed ions. Additionally carbon may be incorporated by radical reactions, electrolyte ionization and field effects [2-4]. This contaminated layer of the oxide finally forms the inner wall of double wall tubes (left). If carbon incorporation and lower quality $TiO_2$ ($H_2O$)-layer can be suppressed, single wall tubes (right) are formed. This inner layer is usually more prone to chemical etching by the anodization electrolyte (mainly fluorides), therefore often the V-shaped inner tube morphology is obtained (as illustrated in the SI Fig. S2).

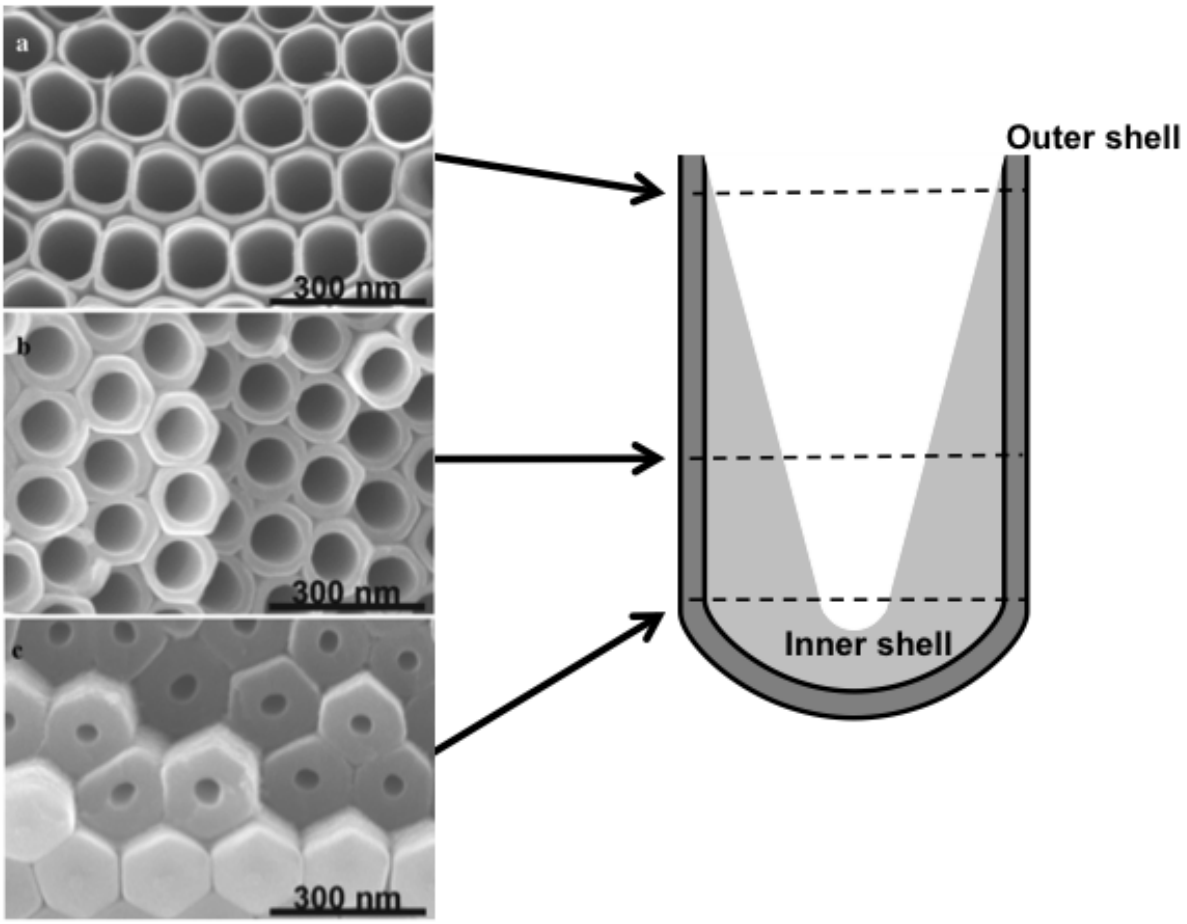


**Fig. S2** SEM images of double wall $TiO_2$ nanotubes [5] and taken from the upper part of the layer (a), in the middle (b) and at the bottom of the layer (c).

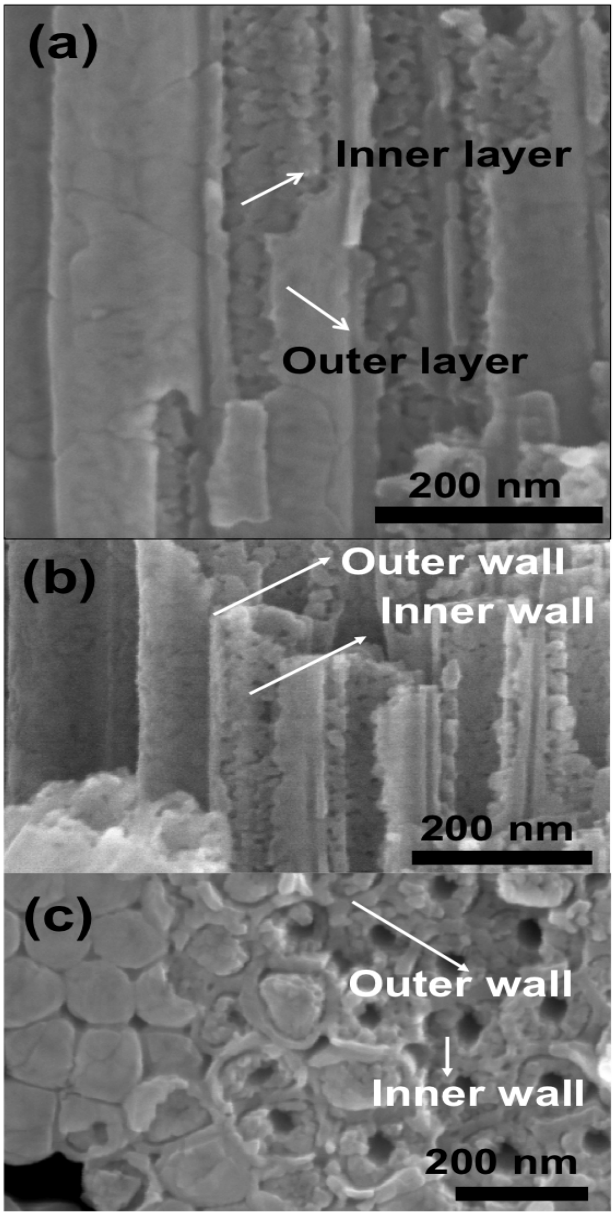


**Fig. S3** Typical morphologies after annealing and cracking double walled samples – showing the partially separated inner, rough oxide layer: (a) side view and (b) bottom view.

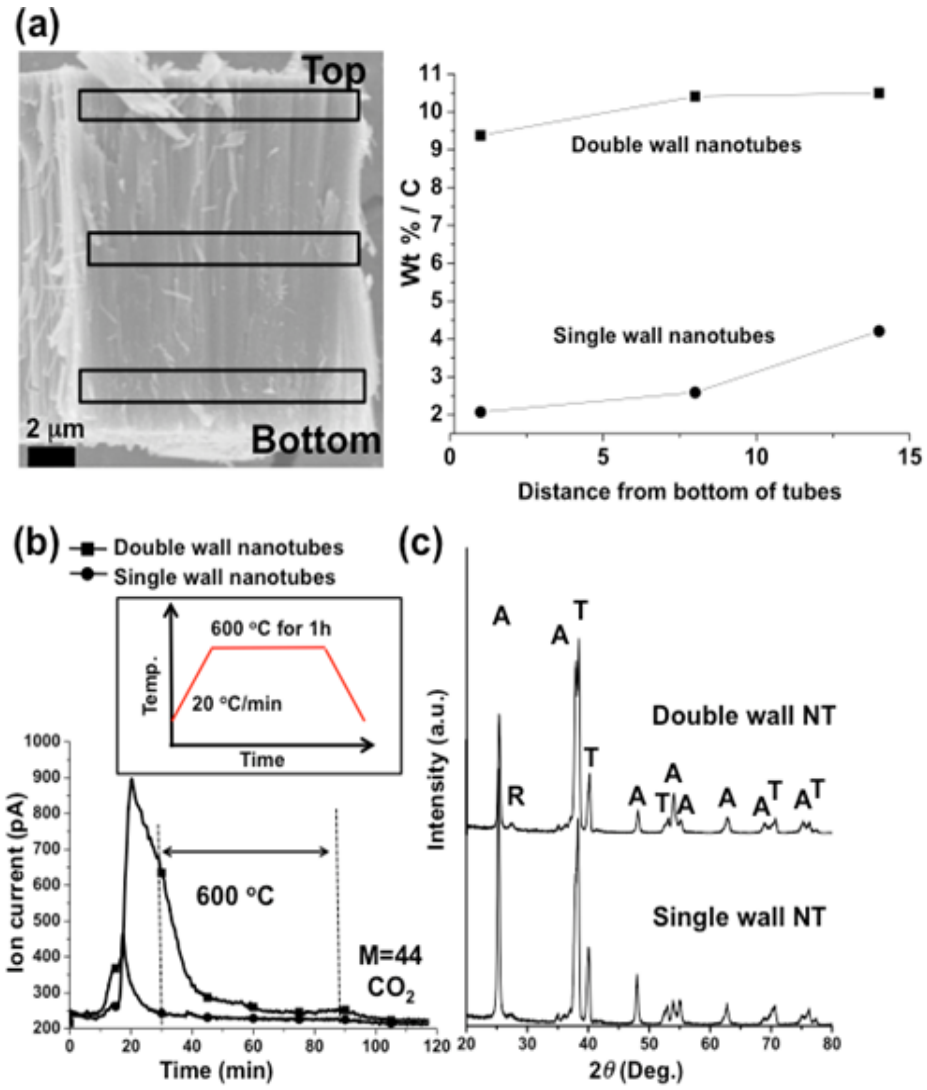


**Fig. S4** (a) SEM image with EDX analysis at 3 different locations (inserted boxes) and summary of the EDX results for C species for the double wall and single wall nanotubes. (b) Thermal desorption profile for M = 44 by TGA-MS analysis for the double wall and single wall TiO2 nanotubes. (c) XRD spectra of the annealed double wall and single wall TiO2 nanotubes (A = anatase, R = rutile and T = titanium).

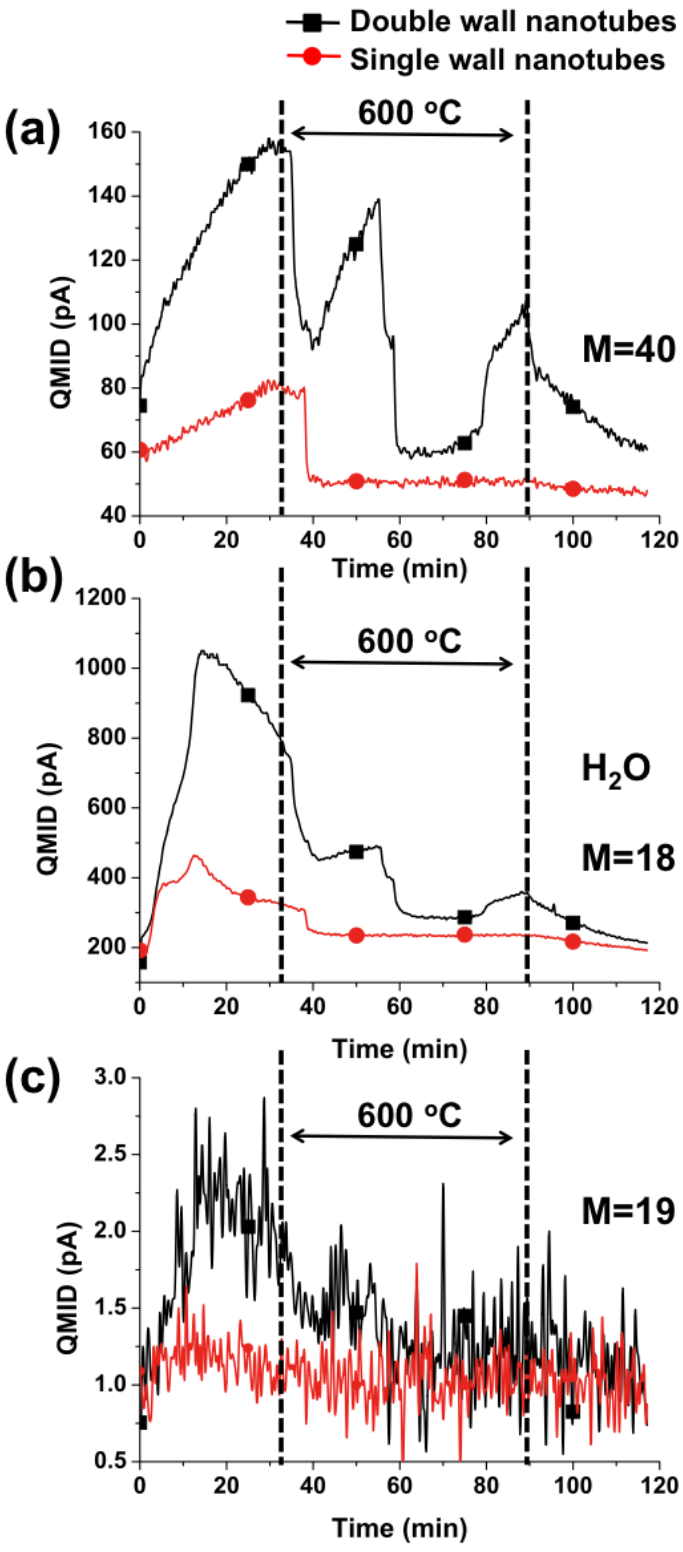


**Fig. S5** The thermal desorption profile for M = 40, 18 and 19 by TGA-MS analysis for double wall and single wall $TiO_2$ nanotubes.

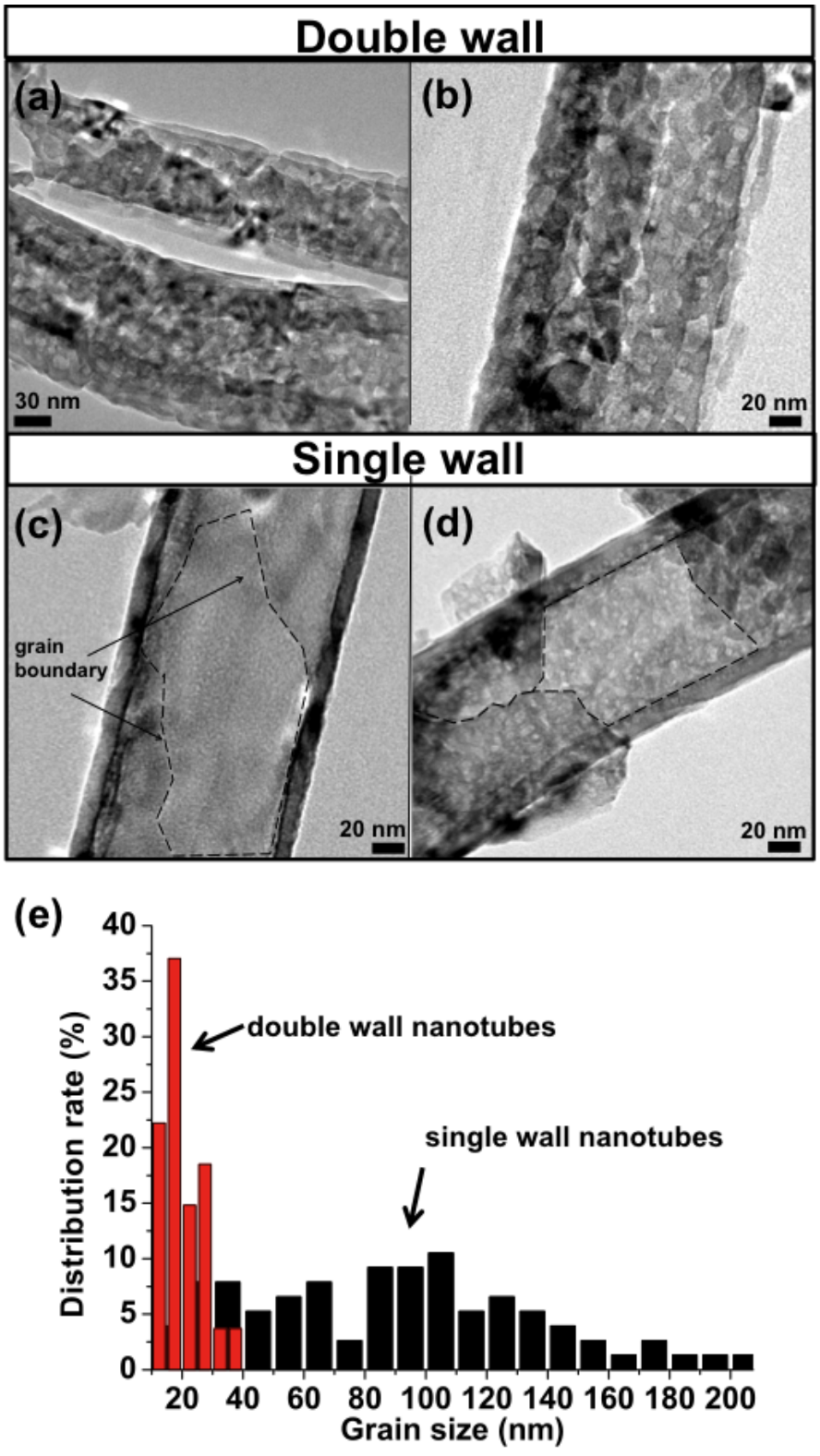


**Fig. S6** TEM images for annealed double wall (a, b) and single wall (c, d) $TiO_2$ nanotubes and the size distribution rate of grains for double wall (red) and single wall (black) $TiO_2$ nanotubes evaluated from > 50 TEM images(e).

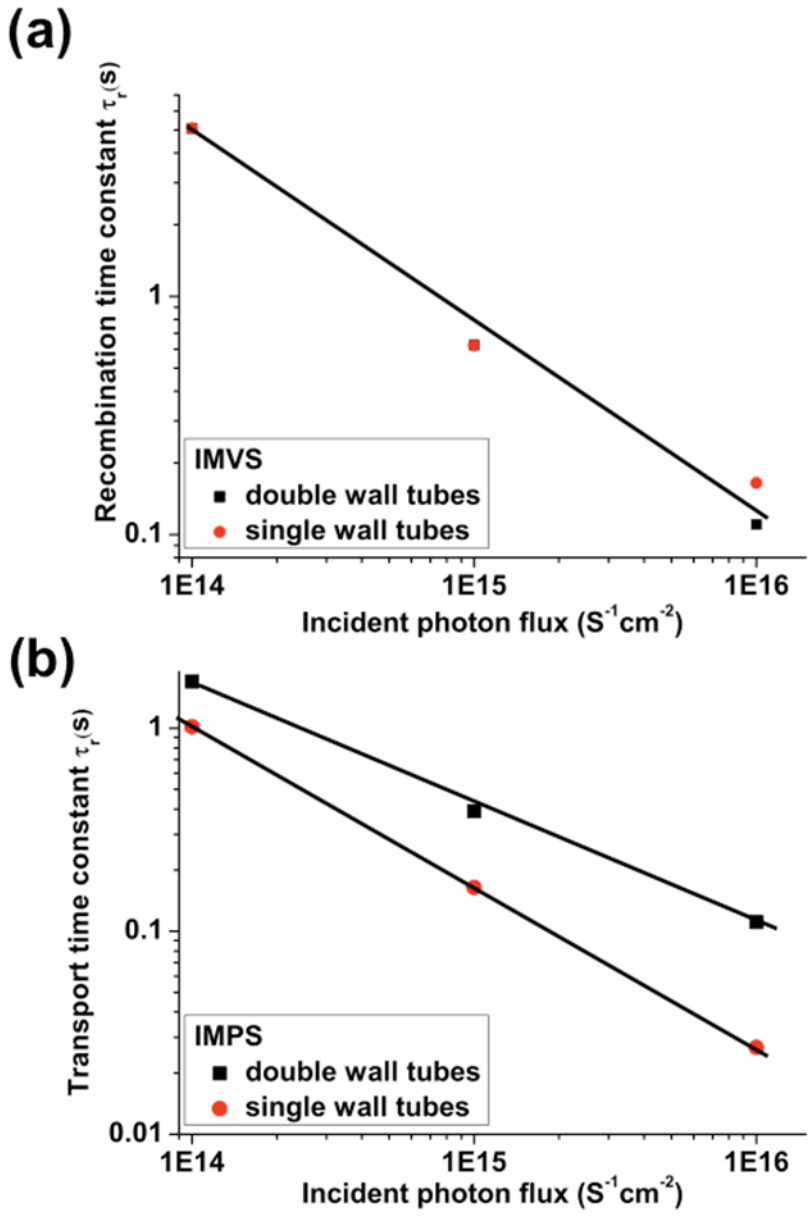


**Fig. S7** Recombination time and transport time constants calculated from IMVS and IMPS for single and double walled DSSCs.

**References:**

[1] C. Fabrega, F. Hernandez-Ramırez, J. D. Prades, R. Jimenez-Dıaz, T. Andreu and J. R. Morante, Nanotechnology, 2010, 21, 445703.

[2] M. Ue, F. Mizutani, S. Takeuchi, and N. Sato, J. Electrochem. Soc., 1997, 144, 3743-3748.

[3] M. Ue, F. Mizutani, S. Takeuchi, and N. Sato, Denki Kagaku, 1997, 65, 1070-1073.

[4] H. Asoh and S. Ono, Materials Science Forum, 2003, 419-422, 957-962.

[5] J. M. Macak, S. P. Albu, and P. Schmuki, Phys. Stat. Sol. (RRL), 2007, 1, 181– 183.